

# Characterizing mechanical properties of three-dimensional printed polylactic acid with variations in nozzle diameter and density via tensile testing for automotive applications

Teuku Edisah Putra<sup>1\*</sup> , Muhammad Dirhamsyah<sup>1</sup>, Amir Zaki Mubarak<sup>1</sup>, Putra Nauli<sup>1</sup>

<sup>1</sup> Department of Mechanical Engineering, Universitas Syiah Kuala, Banda Aceh, Indonesia

\* Corresponding author's e-mail: [edi@usk.ac.id](mailto:edi@usk.ac.id)

## ABSTRACT

This study aimed to identify the mechanical properties of Polylactic Acid. Tensile testing specimens were printed with nozzle diameters of 0.4, 0.6, and 0.8 mm, as well as densities of 10, 50, and 100%, respectively. The results showed that the relationship between stress and strain occurred only in the plastic zone. A nozzle diameter of 0.6 mm with 100% density produced the highest values for all mechanical properties, with an elastic modulus of 1226.2 MPa, ultimate tensile strength of 44.74 MPa, and elongation at the breakpoint of 2.6%. The mechanical properties obtained from the tensile tests were still significantly lower than the native characteristics of Polylactic Acid, which was influenced by moisture due to the porous structure of the fabricated parts. The changes in mechanical properties caused by three-dimensional printing suggested that many parameters should be considered to produce high-quality products.

**Keywords:** polylactic acid, three-dimensional printing, nozzle, density, tensile test, mechanical properties.

## INTRODUCTION

Plastics are widely used across different fields for various purposes since the 20<sup>th</sup> century. According to previous data [1], plastics consumption in Western European countries reached 60 kg/person/year and the United States recorded 80 kg/person/year. Most of the plastics used are synthetic polymers derived from petroleum and their related components [2]. However, petroleum-based products are not environmentally friendly, and the depletion of petroleum reserves is increased by massive consumption [3]. Due to increasing awareness of environmental issues in recent decades, the demand for environmentally friendly materials has risen compared to low-cost, high-strength materials. Therefore, various efforts are continuously implemented to develop alternative materials with a lower environmental impact compared to conventional plastics [2].

Manufacturing industries have rapidly developed to enhance products quality, including

plastics. The conventional process of creating products through subtractive manufacturing methods, which include removing material using machining tools, is increasingly being replaced by additive manufacturing technology such as three-dimensional (3-D) printing. This technology allows for the creation of solid 3-D objects from digital files. Furthermore, 3-D printing has been widely used for generating prototypes and producing spare parts quickly and cost-effectively, while maintaining good quality. The advancement of this technology significantly contributes to various fields and creates new opportunities in production as well as design processes. According to Abadie et al. [4], 40% of material usage could be reduced by 2040 through the use of 3-D printing technology.

In 3-D printing, polylactic acid (PLA) has been identified as a potential material to replace petroleum-based synthetic polymers, which helps to minimize environmental impact [5-7]. It has high biodegradability, breaking down through

natural processes into lactic acid that decomposes to water and carbon dioxide. Furthermore, PLA has thermoplastic properties, allowing it to be melted and reshaped multiple times without significant degradation of mechanical properties. With the rapid advancement in 3-D printing technology in recent years, PLA has been widely used in various fields, such as textiles [6], food [8], healthcare [9], construction [10], and automotive [11]. In the automotive sector, PLA contributes to vehicle manufacturing to withstand loads imposed by passengers, cargo, the surface of the road traversed, as well as weather conditions including wind and rain.

The current challenge in 3-D printing technology is to produce products that are low-cost, quick, and possess good mechanical properties. This raises a significant concern regarding the influence of 3-D printing process on the mechanical properties of PLA. To address the concern, this study was conducted to characterize the mechanical properties of PLA due to the printing process, ensuring suitability for use in automotive components. Tensile tests were performed using specimens of PLA produced through 3-D printing by varying the nozzle diameter and density. Stress-strain curves were obtained after the tensile tests, showing the modulus of elasticity, ultimate tensile strength (UTS), and elongation at the breakpoint. Subsequently, the results were compared to the mechanical properties obtained from injection/compression molding methods. These mechanical properties were expected to serve as a reference regarding the influence of nozzle diameter and density on the mechanical properties of PLA, particularly for automotive applications.

## MATERIALS AND METHODS

### Polylactic acid

PLA is a biopolymer made from agricultural waste such as corn, cassava, sugarcane, and others through carbohydrate fermentation [12]. This process helps reduce environmental pollution and adds value to agricultural activities. Due to the production from renewable resources, the use of PLA decreases dependence on non-renewable fossil fuels, serving as a sustainable alternative to conventional petroleum-based plastics. This makes PLA a suitable option for fields requiring materials that are strong and environmentally friendly.

Carothers et al. [13] were the first to develop PLA using the polymerization and depolymerization of oligomer lactide. In the 1960s, high molecular weight PLA was modified to possess properties similar to petroleum-based plastics. However, commercial production started in 1997 after being developed by Cargill Dow Corporation [14], using a melt processing method to synthesize PLA from its solution [7]. The advantageous characteristics that were identified included biodegradability (naturally decomposes), sustainability, biocompatibility (environmentally friendly), renewability, thermoplasticity, good availability, antibacterial properties, non-toxicity, low density, and high mechanical and thermal properties, as well as cost-effectiveness. The specifications of PLA are presented in Table 1.

As global efforts to protect the environment intensify, awareness of using environmentally friendly materials in the automotive sector is increasing. The use of PLA in the automotive industry holds promising potential due to the acoustic and thermal insulation properties. PLA has been used to manufacture interior components such as dashboards, seat covers, floor mats, door panels, trunk liners, wheel boxes, storage panels, and noise insulation panels. In the future, it is anticipated that the use of PLA in the automotive industries will not be limited to interior components alone, but extend to replacing certain exterior components and body panels [16].

PLA is being developed to become a key material in the automotive sector and make a significant contribution to the sustainability of the industry. Switching to PLA allows car manufacturers to cut down the amount of plastic waste made from

**Table 1.** Specifications of PLA [15]

Parameter	Value
Filament diameter	1.75 mm
Print temperature	190–210 °C
Bed temperature	No heat (60–80)
Density	1.25 g/cm <sup>3</sup>
Heat distortion temperature	56 °C, 0.45 MPa
Melt flow index (g/10 min)	5 (190 C / 2.16 kg)
Tensile strength	65 MPa
Elongation at break	8%
Flexural strength	97 MPa
Flexural modulus	3600 MPa
IZOD impact strength	4 kJ/m <sup>2</sup>

petroleum during the vehicle's lifespan. Moreover, with electric vehicles becoming more common, using this material helps reduce the carbon footprint associated with their production. Because PLA comes from renewable resources and is biodegradable, it is in line with the sustainability goals promoted by electric vehicle manufacturers.

### 3-D printing

According to Gross et al. [17], 3-D printing is a form of additive manufacturing developed by Charles Hull in 1983. Hull created a process called stereolithography, where layers of material were built up gradually using ultraviolet light to cure liquid resin. This innovation paved the way for the development of other 3-D printing methods and applications in various fields, including the automotive sector. The application of 3-D printing allows designers and engineers to produce items more quickly and cost-effectively, without creating expensive injection molds.

Fused deposition modeling (FDM), also called fused filament fabrication (FFF), is the most widely used 3-D printing method due to simplicity, speed, cost-effectiveness, and efficiency. Developed by S. Scott Crump and commercialized in 1990 by Stratasys, as reported by Chennakesava & Narayan [18], FDM works melting thermoplastic material and layering it to create 3-D objects. This method is particularly useful for producing intricate, detailed parts that would have been challenging to make with traditional methods. Additionally, FDM offers great versatility in shaping a wide range of objects, making it suitable for prototyping, modeling, and production [19].

The filament form of PLA is often used in 3-D printing due to low melting point, high strength, low thermal expansion, and good inter-layer adhesion. Other factors contributing to the popularity include ease of use, low toxicity, as well as the ability to produce detailed, accurate,

strong, and neat prints. However, several printing parameters need to be considered, such as nozzle diameter and density, which can affect the mechanical properties of PLA. Adjusting these parameters is crucial to ensure that the quality of printing meets the expected technical specifications for industrial applications.

A potential method to obtain the mechanical properties of a material is through tensile test. Therefore, the PLA filament was used for printing tensile testing specimens in this study. The specimens were modeled using computer-aided design software, as shown in Figure 1, in accordance with ASTM D638-14 [20]. The model was saved into stereo lithography (STL) format to perform the slicing process. This process used the Ultimaker Cura application with the machining parameters shown in Table 2. This process produced G-code which was then transferred to the Creality CX Cartesian 3-D Printing machine. The specification of the machine is listed in Table 3. The digital model was converted into movement data according to the  $x$ ,  $y$ ,  $z$  coordinate system. The model was printed at a printing speed of 60 mm/s using FDM, which printed products through filament extrusion. This process included heating the filament until it melted and softened in the heated liquefier, leading to the melting process. Subsequently, extrusion was performed through a nozzle that moved horizontally and vertically to directly form the object. The nozzle diameters were varied at 0.4, 0.6, and 0.8 mm with densities of 10, 50, and 100%, respectively. The printing process of the specimens is shown in Figure 2.

The principle of 3-D printing using FDM method included applying a layering process, where the object was printed gradually in layers, from the bottom-upward. The machine read the generated G-code of the 3-D design from the the Ultimaker Cura application and assembled the layers sequentially to build a virtual model that was automatically combined to form a complete

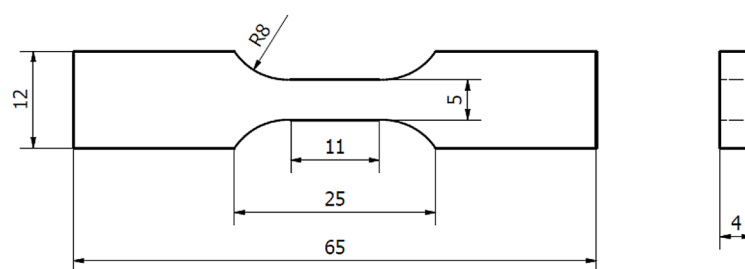


**Figure 1.** Design of the testing specimen (in mm)

**Table 2.** 3-D printing parameters

Material	PLA
Extruder temperature	210 °C
Nozzle diameter	0.4, 0.6, 0.8 mm
Layer thickness	0.2 mm
Density	10%, 50%, 100%

**Table 3.** Specifications of 3-D printing machine

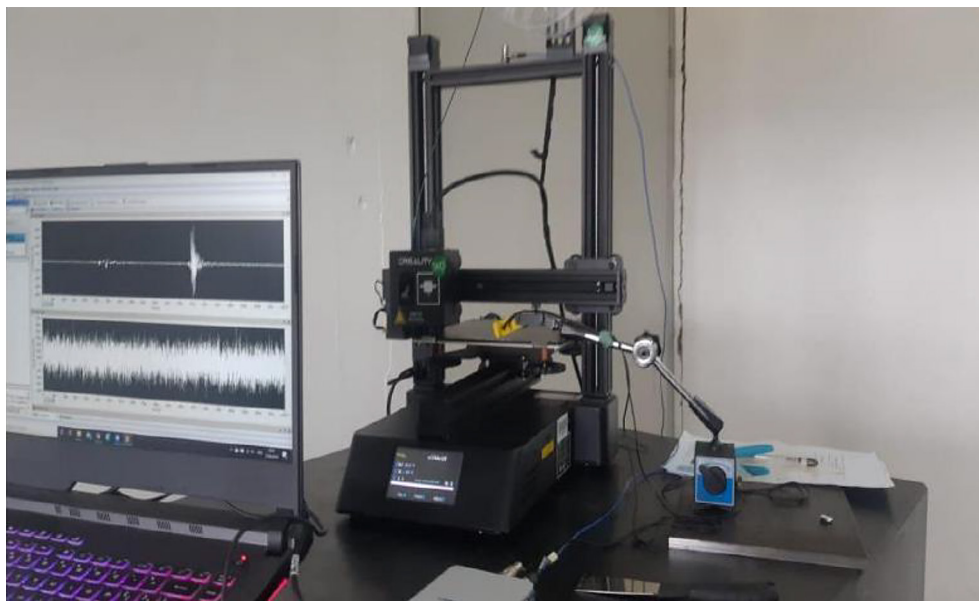
Model	CP - 01
Type	3D Laser, CNC, FDM
Material (frames)	Aluminium extrusion
Platform board	Aluminum alloy, aluminum base
Nozzle diameter	0.4 mm
Nozzle temperature	0 to 260 °C
Product forming size	200 × 200 × 200 mm
Layer thickness	0.1–0.4 mm
LCD screen	Yes
Print speed	10–80 mm/s
Platform/bed temperature	Room temperature to 100 °C

structure. The number of layers in each specimen depended on the nozzle diameter. For a nozzle diameter of 0.4 mm, a total of twelve layers were required (Fig. 3), while nine layers were used for 0.6 mm (Fig. 4). Meanwhile, only eight layers were necessary to form a specimen with a nozzle diameter of 0.8 mm (Fig. 5).

All layers were divided into bottom, middle, and top groups. In the bottom layer, there were four movements, comprising three outer specimens and one inner density movement. Subsequently, the infill density was performed in the middle section after three layers from the bottom, following the grid pattern corresponding to each nozzle size. The middle section consisted of three movements, comprising two outer specimens and one inner density movement. In the top layer, there were also four movements, comprising three outer specimens and one inner density movement. Therefore, there were nine specimens for each nozzle diameter and density combination. Figure 6 shows the printed results obtained from specimens fabricated in accordance with ASTM D638-14 [20], featuring a thickness of 4 mm and a gauge length of 25 mm, which are suitable for tensile testing.

### Tensile test

The mechanical properties of materials need to be determined for application in engineering application due to their influence on strength and formability. This is particularly important for the development of automotive materials, which must withstand loads and pressures under extreme conditions. The mechanical properties considered in this study included modulus of elasticity, UTS, and elongation at the breakpoint. Modulus of elasticity is the resistance of materials to elastic


**Figure 2.** Producing specimens using the Creality CX 3-D printing machine



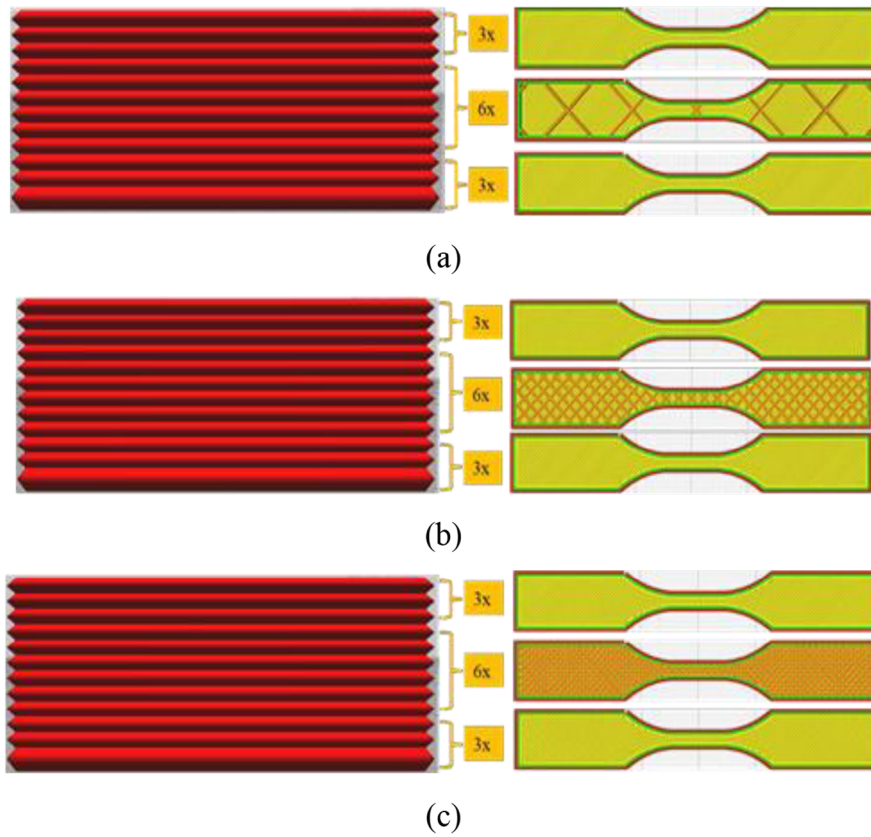


**Figure 3.** Number of layers and nozzle movements for a 0.4 mm diameter nozzle at densities: (a) 10%, (b) 50%, (c) 100%

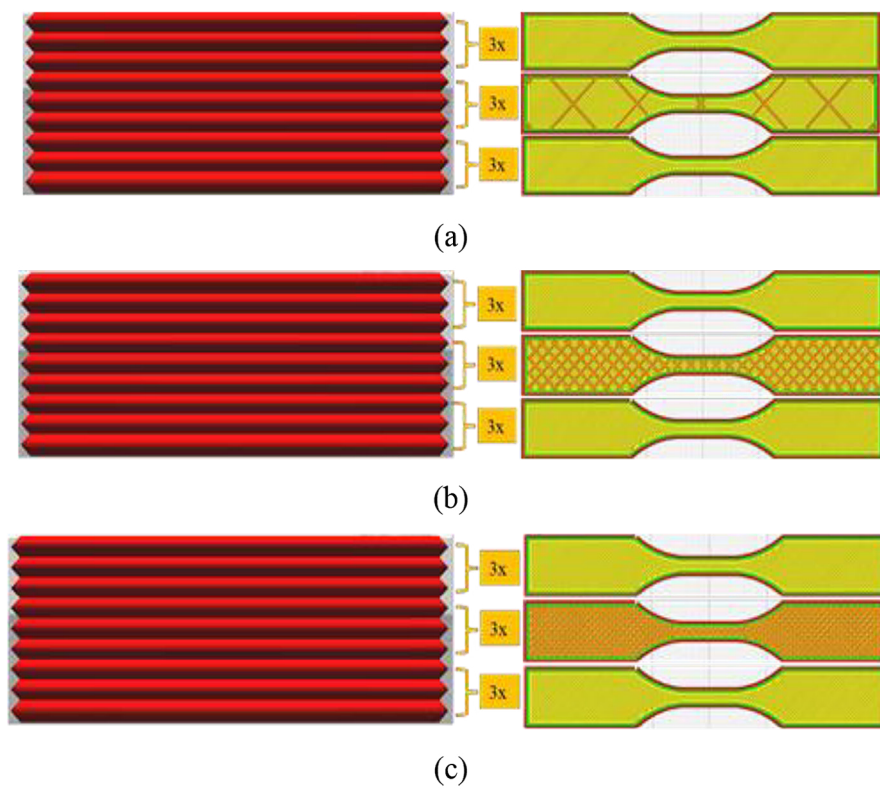


**Figure 4.** Number of layers and nozzle movements for a 0.6 mm diameter nozzle at densities: (a) 10%, (b) 50%, (c) 100%

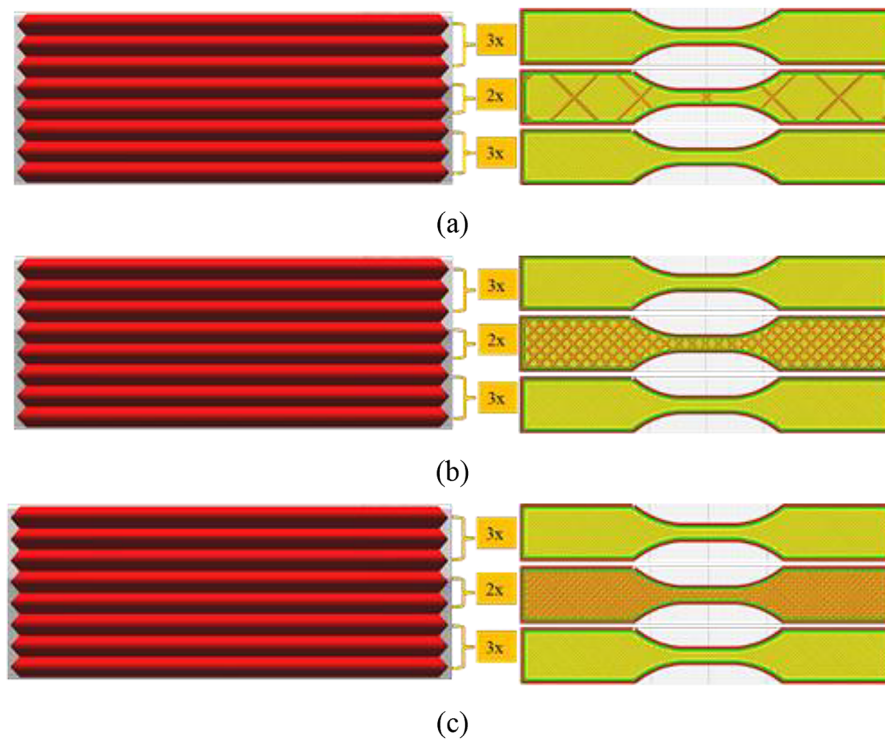


**Figure 5.** Number of layers and nozzle movements for a 0.8 mm diameter nozzle at densities: (a) 10%, (b) 50%, (c) 100%

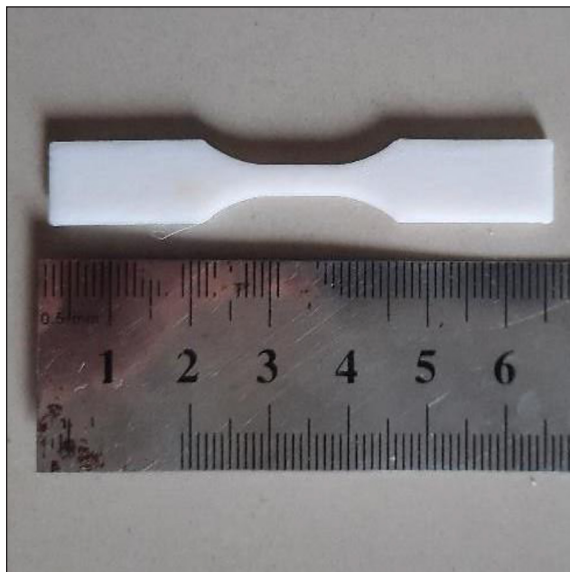


**Figure 6.** Result of specimen printing

deformation when subjected to applied pressure. Understanding the deformation of material under load helps ensure the ability to withstand pressure without experiencing damage. Meanwhile, UTS is the maximum stress that a material can withstand when stretched or pulled before breaking. This is important to ensure the safety as well as sustainability of components. Finally, elongation

at the breakpoint is the percentage increase in length of the material before fracture. Measuring elongation is essential for determining the flexibility of the material, particularly when used in components that are subject to movement.

In this study, the machine used for the tensile test was the Tensilon RTF 1350 with a capacity of 50 kN, suitable for testing fibers, wires, cables, and packaging materials. The test adhered to ASTM D638-14 [20] and was conducted at room temperature, specifically 25 °C. The specimens used were clamped at both ends vertically, as shown in Figure 7. Subsequently, a load was applied gradually at a rate of 10 mm/minute. The specimens experienced deformation characterized by elongation proportional to the gradual increase in tensile load applied uniaxially along both axes of the specimen. After the specimen fractures, a stress-strain curve was obtained. This curve was crucial for understanding the material properties under various operating conditions, particularly in automotive applications.

The stress-strain curve provides the relationship between the stress  $\sigma$  and the strain  $\varepsilon$ , which is expressed as:

$$E = \frac{\sigma}{\varepsilon} \quad (1)$$



Figure 7. Specimen on the tensile testing machine

where:  $E$  is the modulus of elasticity. Stress  $\sigma$  is obtained by dividing the applied load  $F$  acting perpendicular to the cross-section through the original cross-sectional area  $A_0$  before loading, with the equation expressed as:

$$\sigma = \frac{F}{A_0} \quad (2)$$

Strain  $\varepsilon$  can be determined using this equation:

$$\varepsilon = \frac{\Delta L}{L_0} \quad (3)$$

where:  $\Delta L$  is the change in length and  $L_0$  is the original length before the load is applied.

## RESULTS AND DISCUSSION

Figures 8-10 show the stress-strain curves obtained from tensile tests for nozzles with diameters of 0.4 mm, 0.6 mm, and 0.8 mm at densities of 10, 50, and 100%, respectively. For the 0.4 mm nozzle, the curve indicated a maximum modulus of elasticity of 1,166 MPa and UTS of 38.85 MPa at 100% density. However, the maximum elongation was achieved at 10% density, reaching 2.2%. For the 0.6 mm nozzle, all maximum values were observed at 100% density,

with modulus of elasticity at 1,226.2 MPa, UTS 44.74 MPa, and elongation of 2.6%. Similarly, for the 0.8 mm nozzle, all maximum values were also recorded at 100% density, with a modulus of elasticity at 1,207.5 MPa, UTS 42.09 MPa, and elongation of 2.2%. Results of conducted tensile tests showed that the influence of nozzle diameter and density in 3-D printing was highly significant in determining the mechanical properties of the products.

The stress-strain relationship of PLA includes both elastic and plastic regions. The yield strength corresponds to the stress level at which plastic deformation begins. Regarding the individual mechanical properties, the highest modulus of elasticity was shown by the 0.6 mm nozzle at 100% density, measuring 1,226.2 MPa, as presented in Figure 11. Compared to the modulus of elasticity at densities of 50 and 100%, which tended to increase with rising density, the value at 10% density decreased but without significant changes.

From Figure 12, the highest UTS was provided by the 0.6 mm nozzle at 100% density, measuring 44.74 MPa. The UTS at 10% density tended to decrease as density increased, similar to the behavior observed in the modulus of elasticity. However, the UTS values at 50 and 100% density did not show consistent conditions. The 0.6 mm nozzle at 100% density also yielded the maximum elongation of 2.6%, as shown in Figure 13. Similar to the UTS values, the elongation at 10% density also tended to decrease with increasing density, while the elongation at 50 and 100% density did not provide consistent results.

From the results, a nozzle diameter of 0.6 mm with 100% density provided maximum values for all mechanical properties. This showed that the quality of interlayer bonding in the specimens could be achieved with a 0.6 mm diameter nozzle. The quality of interlayer bonding was crucial for manufacturers of automotive components searching for a balance between production costs and material performance. In addition, the material's density played an important role in determining its strength. Higher-density specimens generally exhibited greater strength, likely due to reduced internal porosity and a more compact structure that allowed the material to better resist applied loads and stress. These results were in line with previous reports showing that mechanical properties depended on the parameters of the printing process [21-22], such as nozzle diameter [23-24] and density [25].

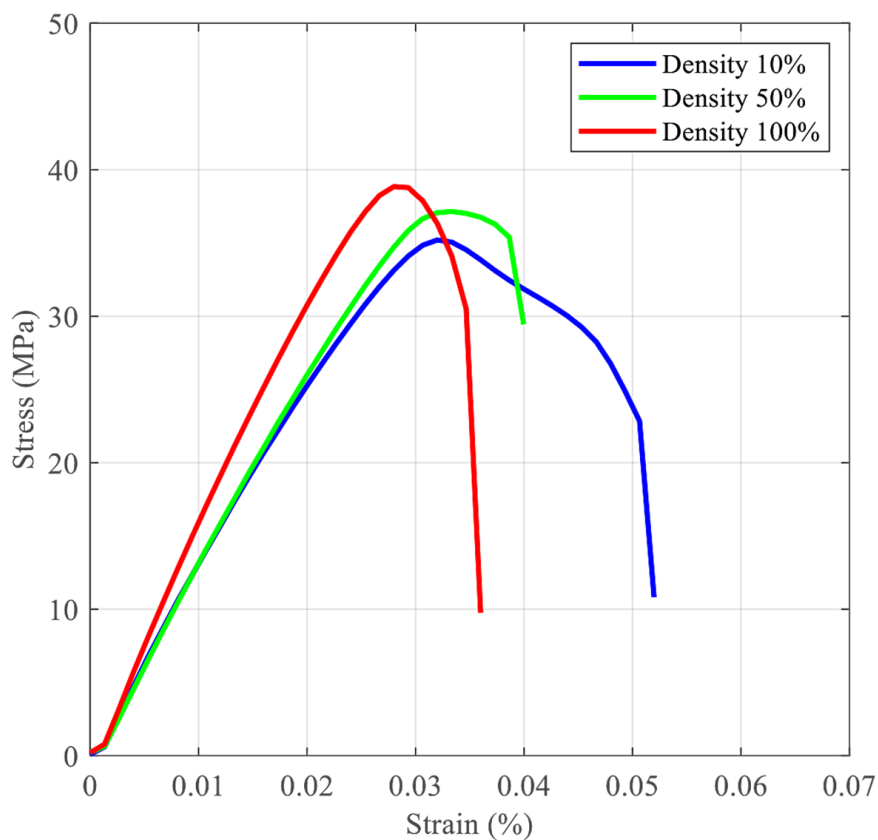


**Figure 8.** Stress-strain curves for a 0.4 mm diameter nozzle at each density

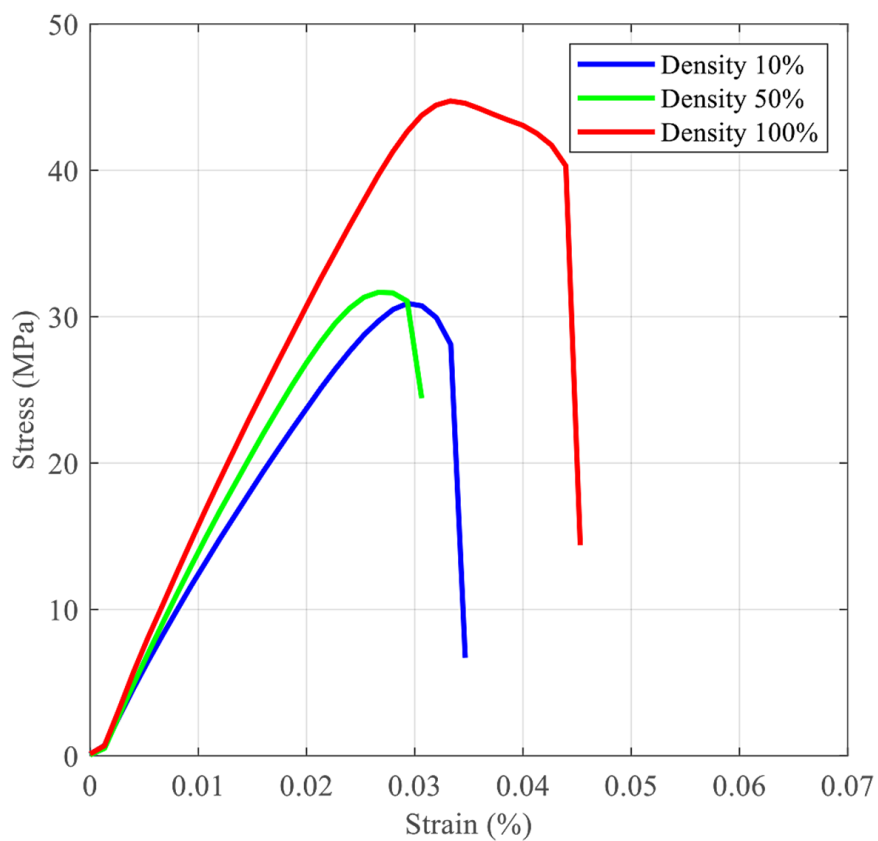


**Figure 9.** Stress-strain curves for a 0.6 mm diameter nozzle at each density



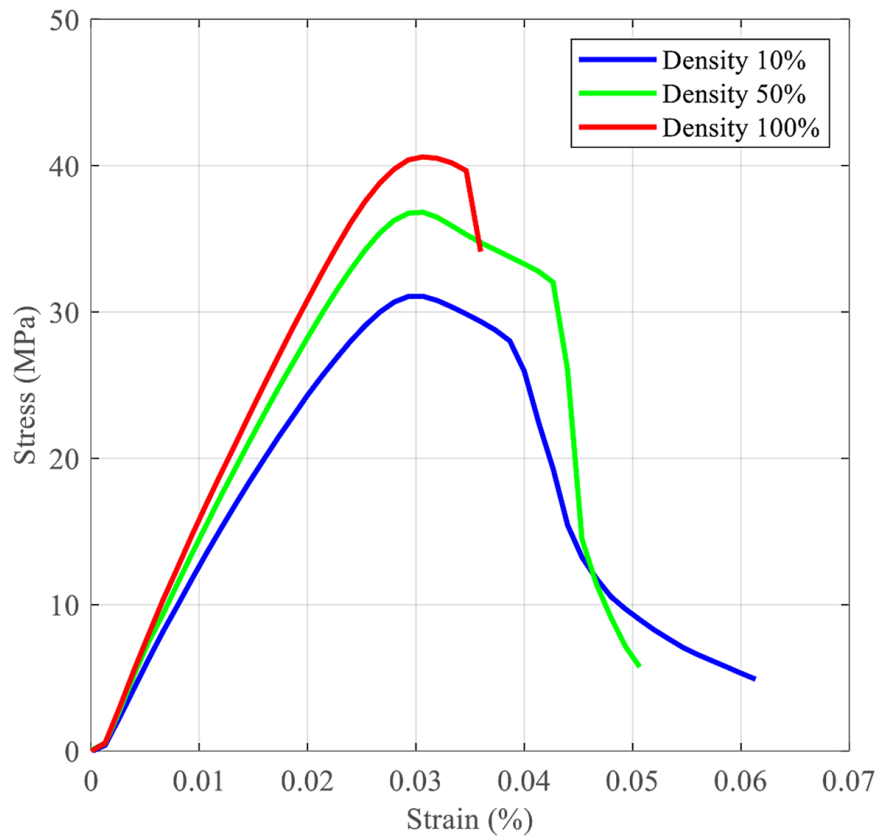


**Figure 10.** Stress-strain curves for a 0.8 mm diameter nozzle at each density

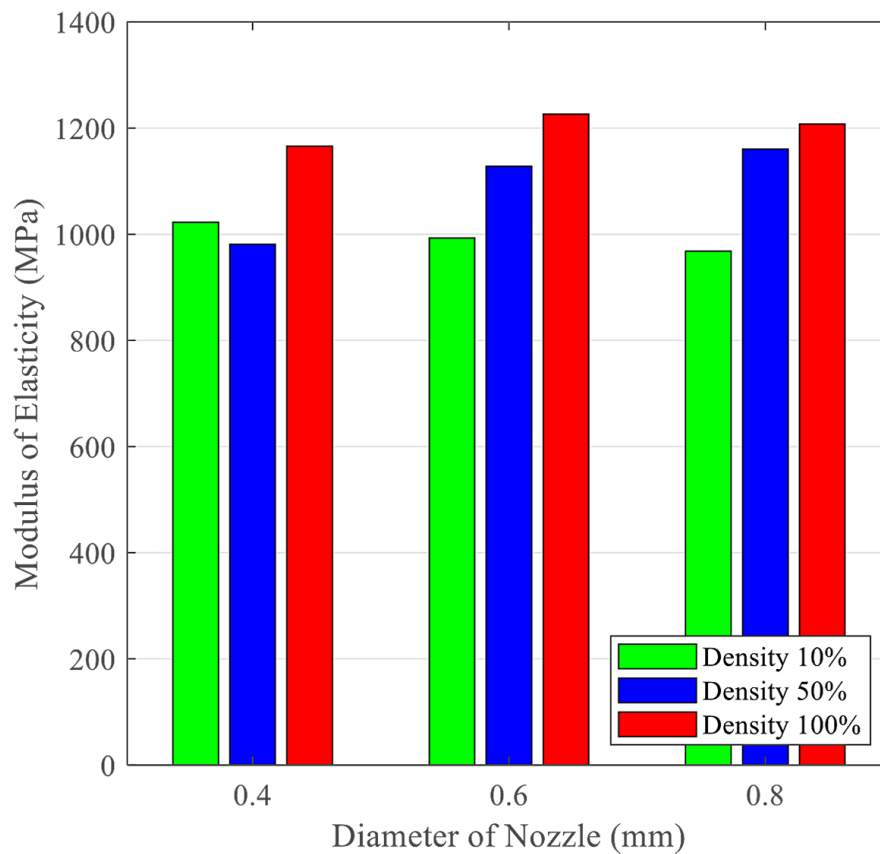


**Figure 11.** Comparison of modulus of elasticity for each nozzle diameter and density

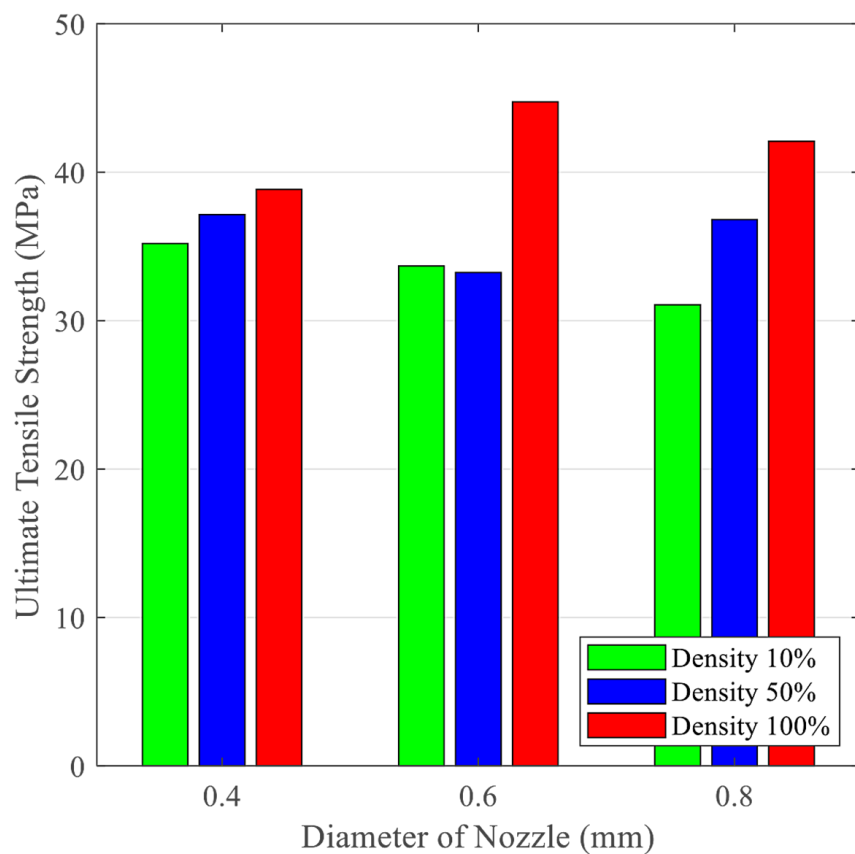


**Figure 12.** Comparison of UTS for each nozzle diameter and density

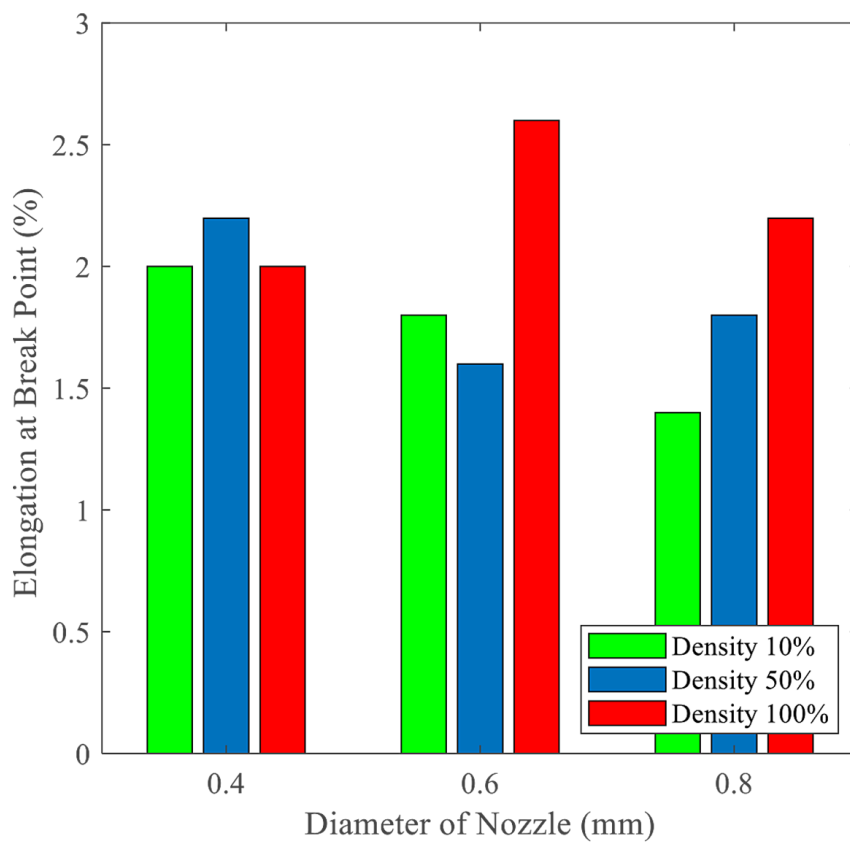


**Figure 13.** Comparison of elongation at break point for each nozzle diameter and density

Despite the significant correlation, the values were significantly below the native mechanical properties of PLA, as shown in Table 1. The maximum modulus of elasticity from the printing results was 1,226.2 MPa, which was only 34% of the original. The obtained UTS was 44.74 MPa, which was only 46% compared to the original. Meanwhile, the maximum elongation was only 2.6%, significantly lower than the original, which could reach approximately 8%. The significant difference in mechanical properties of PLA between injection/compression molding and 3-D printing methods was influenced by moisture due to the porous structure of the fabricated parts. Moisture is one of the main challenges that must be addressed in the 3-D printing process to ensure optimal strength. This is because moisture-absorbing PLA filaments lead to poor print quality, including a reduction in mechanical strength. Moisture can also cause a plasticization effect, which decreases the mechanical strength of the processed polymers.

## CONCLUSIONS

In conclusion, this study investigated the effects of nozzle diameter and density on the mechanical properties of 3-D printed PLA for automotive applications. Tensile test specimens were printed using FDM technology with nozzle diameters of 0.4, 0.6, and 0.8 mm, and densities of 10, 50, and 100%. The results showed that the relationship between stress and strain occurred only in the plastic zone. Additionally, the quality of inter-layer bonding in the specimens could be achieved with a nozzle diameter of 0.6 mm. Materials with higher density tended to have greater strength because a larger mass per volume provided more material to withstand loads and stress. The 0.6 mm nozzle at 100% density showed a modulus of elasticity of 1,226.2 MPa, UTS of 44.74 MPa, and elongation of 2.6%. The mechanical properties obtained from these tensile tests were significantly below the native mechanical properties of PLA, influenced by moisture due to the porous structure of the fabricated parts. Therefore, many parameters should be considered to ensure that the product's strength can withstand the loads. These results provided important insights for the automotive industry focusing on optimizing the use of PLA in the 3-D printing process for components that required high strength and durability.

## Acknowledgments

The authors express gratitude to Universitas Syiah Kuala for financial support through grant no. 159/UN11.2.1/PG.01.03/SPK/PTNBH/2024.

## REFERENCES

1. Ahvenainen R. *Modern Plastics Handbook*. 1st ed. Woodhead Publishing Limited; 2003.
2. Raddadi N, Fava F. Biodegradation of oil-based plastics in the environment: existing knowledge and needs of research and innovation. *Sci Total Environ*. 2019; 679: 148–58.
3. Sid S, Mor RS, Kishore A, Sharanagat VS. Bio-sourced polymers as alternatives to conventional food packaging materials: a review. *Trends Food Sci Technol*. 2021; 115(1): 87–104.
4. Abadie A, Diamond A, Hainmueller J. Synthetic control methods for comparative case studies: estimating the effect of California's tobacco control program. *J Am Stat Assoc*. 2010; 105(490): 493–505.
5. Rajeshkumar G, Seshadri SA, Devnani GL, Sanjay MR, Siengchin S, Maran JP, et al. Environment friendly, renewable and sustainable poly lactic acid (PLA) based natural fiber reinforced composites - a comprehensive review. *J Clean Prod*. 2021; 310: 127483.
6. Tripathi N, Misra M, Mohanty AK. Durable polylactic acid (PLA)-based sustainable engineered blends and biocomposites; recent developments, challenges, and opportunities. *ACS Eng Au*. 2021; 1: 7–38.
7. Trivedi AK, Gupta MK, Singh H. PLA based biocomposites for sustainable products: a review. *Adv Ind Eng Polym Res*. 2023; 6(4): 382–95.
8. Nazrin A, Sapuan SM, Zuhri MYM, Ilyas RA, Syafiq R, Sherwani SFK. Nanocellulose reinforced thermoplastic starch (TPS), polylactic acid (PLA), and polybutylene succinate (PBS) for food packaging applications. *Front Chem*. 2020; 8: 213.
9. Castañeda-Rodríguez S, González-Torres M, Ribas-Aparicio RM, Prado Audelo MLD, Leyva Gómez G, Güler ES, et al. Recent advances in modified poly (lactic acid) as tissue engineering materials. *J Biol Eng*. 2023; 17(1).
10. Morales AP, Güemes A, Fernandez-Lopez A, Valero VC, Llano SCLR. Bamboo-poly(lactic acid) (PLA) composite material for structural applications. *Materials (Basel)*. 2017; 10(11): 1286.
11. Khodabakhshi K. Automotive Applications: Polylactic Acid and Biocomposite Parts. In: *Encyclopedia of Polymer Applications*. CRC Press; 2019.
12. Ilyas RA, Sapuan SM, Harussani MM, Hakimi MYAY, Haziq MZM, Atikah MSN, et al. Polylactic

- acid (PLA) biocomposite: processing, additive manufacturing and advanced applications. *Polymers (Basel)*. 2021; 13(8): 1326.
13. Carothers WH, Dorough GL, Natta FJ. Studies of polymerization and ring formation. X. The reversible polymerization of six-membered cyclic esters. *J Am Chem Soc*. 1932; 54(2): 761–772.
14. Dorgan JR, Braun B, Wegner JR, Knauss DM. Poly (lactic acids): a brief review. *ACS Symp Ser*. 2006; 939: 102–125.
15. Pantani R, Volpe V, Titomanlio G. Foam injection molding of poly (lactic acid) with environmentally friendly physical blowing agents. *J Mater Process Technol*. 2014; 214(12): 3098–3107.
16. Bouzouita A. Elaboration of polylactide-based materials for automotive application: study of structure-process-properties interactions [thesis]. Université de Mons; 2016.
17. Gross BC, Erkal JL, Lockwood SY, Chen C, Spence DM. Evaluation of 3D printing and its potential impact on biotechnology and the chemical sciences. *Anal Chem*. 2014; 86(7): 3240–3253.
18. Chennakesava P, Narayan YS. Fused deposition modeling – insights. In: *International Conference on Advances in Design and Manufacturing (ICAD&M'14)*. 2014; 1345–1350.
19. Yang L, Li S, Li Y, Yang M, Yuan Q. Experimental investigations for optimizing the extrusion parameters on FDM PLA printed parts. *J Mater Eng Perform*. 2019; 28(1): 169–182.
20. ASTM D638-14. Standard Test Method for Tensile Properties of Plastics. ASTM International; 2014.
21. Dave HK. Compressive strength of PLA based scaffolds: effect of layer height, infill density and print speed. *Int J Mod Manuf Technol*. 2019; 11(1): 21–27.
22. Dey A, Yodo N. A systematic survey of FDM process parameter optimization and their influence on part characteristics. *J Manuf Mater Process*. 2019; 3(64): 1–30.
23. Kaveh M, Badrossamay M, Foroozmehr E, Etefagh AH. Optimization of the printing parameters affecting dimensional accuracy and internal cavity for HIPS material used in fused deposition modeling processes. *J Mater Process Technol*. 2015; 226: 280–286.
24. Tlegenov Y, Hong GS, Lu WF. Nozel condition monitoring in 3D printing. *Robot Comput Integr Manuf*. 2018; 54: 45–55.
25. Fernandez-Vicente M, Calle W, Ferrandiz S, Conejero A. Effect of infill parameters on tensile mechanical behavior in desktop 3D printing. *3D Print Addit Manuf*. 2016; 3(3): 183–192.